



## Estimation of Michaelis–Menten constant of efflux transporter considering asymmetric permeability

Kiyohiko Sugano<sup>a,\*</sup>, Yoshiyuki Shirasaka<sup>b,1</sup>, Shinji Yamashita<sup>b</sup>

<sup>a</sup> Global Research & Development, Sandwich Laboratories, Research Formulation, Pfizer Inc., CT13 9NJ, Sandwich, Kent, UK

<sup>b</sup> Faculty of Pharmaceutical Sciences, Setsunan University, Nagaotoge-cho 45-1, Hirakata, Osaka 573-0101, Japan

### ARTICLE INFO

#### Article history:

Received 26 November 2010

Received in revised form 15 March 2011

Accepted 24 March 2011

Available online 8 April 2011

#### Keywords:

Passive diffusion

Transporter

Asymmetric

Efflux

Mechanistic model

### ABSTRACT

It was previously reported that the apparent  $K_m$  values of P-gp in apical to basal (A to B) and basal to apical (B to A) directions were different. The purpose of the present study was to derive a theoretical framework by which this asymmetric concentration–permeability profile can be explained using a single intrinsic  $K_m$  value. A three compartment model was used to represent the apical, cytosol and basal compartments. The difference of passive permeability and the surface areas between the apical and basolateral membrane were explicitly taken into account. Applying the steady state approximation and considering the mass balance in the cytosol compartment, an open analytical solution was obtained. By using this equation, the asymmetric concentration–permeability profile was appropriately reproduced. In addition, the expression level dependency of apparent  $K_m$  was also reproduced.

© 2011 Elsevier B.V. All rights reserved.

### 1. Introduction

The passive diffusion and carrier mediated transport coexist in biological membrane permeation of a drug (Sugano et al., 2010). For appropriate drug design, clinical PK prediction, and a clinical use of a drug, it is important to understand the contribution and interplay of these factors. A fully mechanistic molecular-level physiologically based pharmacokinetic model is required to quantitatively evaluate the contributions of these factors. There have been many extensive investigations following this approach (Garmire et al., 2007; Garmire and Hunt, 2008; Kwon et al., 2004; Rostami-Hodjegan and Tucker, 2007; Yang et al., 2007). One of the critical factors for this approach is to obtain intrinsic kinetic parameters for carrier mediated transport such as intrinsic  $K_m$  and  $J_{max}$ . (In this article,  $K_m$  refers to intrinsic  $K_m$  based on free cytosol concentration unless otherwise noted.) However, apparent  $K_m$  and  $J_{max}$  which are based on the donor chamber concentration have usually been obtained from experimental apparent permeability data. It was previously reported that the apparent  $K_m$  values of P-gp in apical to basal (A–B) and basal to apical (B–A) directions are different (Troutman and Thakker, 2003a). In addition, apparent  $K_m$  was

found to be dependent on the expression level of P-gp (the intrinsic  $K_m$  should be consistent) (Horie et al., 2003; Shirasaka et al., 2008). One of the reasons for these two observations was suggested to be that the unbound drug concentration in the cytosol is not equal to that in the donor compartment (Korjamo et al., 2007). In addition, the reason for the apparent  $K_m$  being asymmetric values was suggested to be the difference in passive permeability between apical and basal membranes. This point was previously demonstrated by computational simulation studies using virtual drugs (Korjamo et al., 2007). However, in these simulation studies, the intrinsic  $K_m$  and  $J_{max}$  values of a real drug have not been obtained from the experimental data.

Recently, Tachibana et al. reported a simple equation to calculate the steady state permeability considering the effect of an efflux transporter in the apical membrane (Tachibana et al., 2010). They successfully explained the expression level dependency of apparent  $K_m$  and the intrinsic  $K_m$  values of 3 P-gp substrates were obtained (Tachibana et al., 2010). The purpose of the present study was to extend their approach to handle the difference of apical and basolateral permeation.

Even though a 3 compartment model (Fig. 1), i.e., apical, cytosol and basolateral compartments, has been employed to represent the epithelial cell membrane in many reports, little is known about the difference of passive trans-membrane diffusion in the apical and basolateral membrane and its effect on experimentally observable apparent permeability. Previously, it was assumed that the apical and basolateral membranes have the same surface area and pas-

\* Corresponding author. Tel.: +44 1304 644338.

E-mail address: [Kiyohiko.Sugano@pfizer.com](mailto:Kiyohiko.Sugano@pfizer.com) (K. Sugano).

<sup>1</sup> Present address: Faculty of Pharmacy, Institute of Medical, Pharmaceutical and Health Sciences, Kanazawa University, Kakuma, Kanazawa 920-1192, Japan.

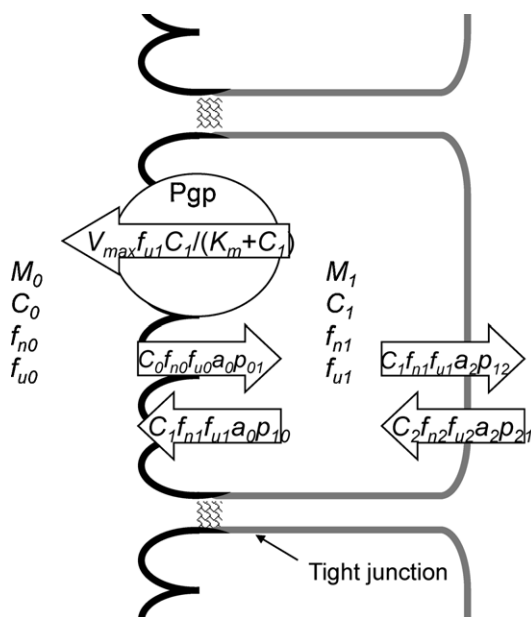


Fig. 1. Schematic presentation of epithelial cell.

sive permeability (Heikkinen et al., 2010; Tachibana et al., 2010). In this report, a model equation to calculate the apparent membrane permeability of a drug across a cell monolayer with an efflux transporter in the apical membrane is first derived, considering the difference of the permeability–surface area products in the apical and basolateral membranes. This theoretical model revealed some characteristics of membrane permeability which could be originated from the difference of passive apical and basolateral permeation. This equation was then applied to analyze experimental data of concentration dependent A–B and B–A permeation of P-gp substrates.

## 2. Equations

Theoretical equations for ideal/absolute intrinsic parameters are first derived. However, the ideal/absolute intrinsic permeability data cannot be directly obtained from the experimental data since an exact surface area of monolayer cells is difficult to obtain. Therefore, the ideal parameters are replaced with practical ones which are experimentally obtainable using a key equation of Eq. (3). By employing this step-wise sequence, the meaning of each parameter is explicitly understood.

### 2.1. Equations using ideal parameters

The three compartment model was used to express the apical, cytosol and basolateral compartments (compartment 0–2, respectively)(Fig. 1) in similar to the previous theoretical studies (Korjamo et al., 2007). The mass balance of a drug in the cytosol is the sum of carrier-mediated and passive trans-bilayer transports of the drug for both influx and efflux directions from/into apical and basolateral compartments. When the efflux transporter is located on the apical membrane, the mass balance in the cytosol is written as:

$$\frac{dM_1}{dt} = C_0f_{n0}f_{u0}a_0p_{01} - C_1f_{n1}f_{u1}a_0p_{10} - C_1f_{n1}f_{u1}a_2p_{12} + C_2f_{n2}f_{u2}a_2p_{21} - \frac{V_{max}C_1f_{u1}}{K_m + C_1f_{u1}} \quad (1)$$

where  $f_n$  is the fraction of the neutral charge form of drug molecules (dependant on pH and  $pK_a$  of a drug) (in the following, the number

in the subscript indicates the compartment),  $f_u$  is the free unbound fraction,  $p$  (lower-case letter) is ideal passive permeability of undissociated molecules (the sequence number in the subscript indicates the direction, i.e.,  $p_{01}$  corresponds to permeation from 0 to 1 compartment (Fig. 1)),  $C$  is total dissolved drug concentration in each compartment,  $a$  is the absolute surface area of the cell membrane,  $M$  is the amount of a drug in each compartment and  $K_m$  is the intrinsic Michaelis–Menten constant. In Eq. (1), the pH partition and free fraction theories were assumed. When the pH values in all compartments are the same (i.e.,  $f_{n0} = f_{n1} = f_{n2}$ ) (e.g., pH 7.4) and no additive is used in the apical and basolateral side ( $f_{u0} = f_{u2} = 1$ ), Eq. (1) can be simplified to:

$$\frac{dM_1}{dt} = C_0a_0p_{PD} - C_1f_{u1}a_0p_{PD} - C_1f_{u1}a_2\alpha p_{PD} + C_2a_2\alpha p_{PD} - \frac{V_{max}C_1f_{u1}}{K_m + C_1f_{u1}} \quad (2)$$

In this equation, it was assumed that passive diffusion of a neutral molecular species across a lipid bilayer membrane is symmetric in the influx and efflux directions, whereas apical and basolateral membrane could show different permeability ( $f_{n0}p_{01} = f_{n1}p_{10} = p_{PD}$ ,  $f_{n1}p_{12} = f_{n2}p_{21} = \alpha p_{PD}$ ) (see Appendix).  $\alpha$  was introduced to reflect the ratio of passive permeability between the apical and basolateral membranes.

### 2.2. Converting the equation with the ideal parameters to that with the practically available parameters

Since we cannot observe an ideal intrinsic passive permeability and absolute membrane surface area, we have to convert the ideal parameters to observable (apparent) parameters. Apparent passive transcellular diffusion under a perfect inhibition of the transporters ( $P_{app,PD,trans}$ ) usually collapses to the same value in both A–B and B–A directions. Usually apparent permeability values are practically defined based on the flat surface area of a cell culture well ( $A_{well}$ ). On the other hand, when considering the real cell structure, the A to B permeation is a sequential permeation through the apical and basolateral membranes. Therefore,  $p_{PD}$  can be expressed as,

$$p_{PD} = A_{well} \frac{a_0 + a_2\alpha}{\alpha a_0 | a_2} P_{app,PD,trans} \quad (cf. \quad A_{well} P_{app,PD,trans} = \left( \frac{1}{a_0} + \frac{1}{\alpha a_2} \right)^{-1} p_{PD}) \quad (3)$$

This equation is the key for converting observable permeability values to ideal ones.  $P_{app,PD,trans}$  can be calculated by subtracting the contribution of paracellular pathway permeability ( $P_{para}$ ) from in vitro apparent permeability.  $P_{para}$  can be calculated from the molecular weight and  $pK_a$  of a drug as previously reported (Saitoh et al., 2004; Sugano, 2009; Sugano et al., 2002). By inserting the key equation of Eq. (3) into Eq. (2) and considering the mass balance at a steady state, we obtain:

$$C_0a_0^* - C_1f_{u1}a_0^* - C_1f_{u1}a_2^* + C_2a_2^* - \left( \frac{1}{a_2^*} + \frac{1}{a_0^*} \right)^{-1} P_{app,PD,trans}^{-1} \frac{J_{max,app}C_1f_{u1}}{K_m + C_1f_{u1}} = 0 \quad (4)$$

$$a_0^* = \frac{a_0}{a_0 + \alpha a_2}, \quad a_2^* = \frac{\alpha a_2}{a_0 + \alpha a_2}, \quad V_{max} = A_{well} J_{max,app} \quad (5)$$

By solving Eq. (4) for  $C_{1f_{u1}}$  (this is a quaternary equation of  $C_{1f_{u1}}$ . See Appendix Eq. (A-2)), the free drug concentration in the cell compartment ( $C_{1f_{u1}}$ ) can be calculated as,

$$C_{1f_{u1}} = \frac{-b + \sqrt{b^2 - 4c}}{2} \quad (6)$$

$$b = K_m - (C_0 a_0^* + C_2 a_2^*) + \left( \frac{1}{a_0^*} + \frac{1}{a_2^*} \right)^{-1} P_{app,PD,trans}^{-1} J_{max,app} \quad (7)$$

$$c = -K_m(C_0 a_0^* + C_2 a_2^*) \quad (8)$$

By definition, apparent epithelial membrane permeability ( $P_{app,ep}$ , paracellular pathway neglected) can be expressed as,

$$P_{app,ep,A-B} = \frac{\alpha a_2}{A_{well}} \frac{C_{1f_{u1}}}{C_0} p_{PD} = \frac{1}{a_0^*} \frac{C_{1f_{u1}}}{C_0} P_{app,PD,trans} \quad (9)$$

$$\begin{aligned} P_{app,ep,B-A} &= \frac{\alpha a_2}{A_{well}} \left( 1 - \frac{C_{1f_{u1}}}{C_2} \right) p_{PD} \\ &= \frac{1}{a_0^*} \left( 1 - \frac{C_{1f_{u1}}}{C_2} \right) P_{app,PD,trans} \end{aligned} \quad (10)$$

By inserting  $C_{1f_{u1}}$  (Eq. (6)) into Eqs. (9) and (10),  $P_{app,ep}$  at a donor compartment concentration ( $C_0$  or  $C_2$ ) can be calculated from  $K_m$  and  $J_{app,max}$  via calculation of  $C_{1f_{u1}}$ . It should be emphasized that  $C_{1f_{u1}}$  is the unbound drug concentration and information about the free fraction in the cytosol ( $f_{u1}$ ) is not a necessarily prerequisite datum for this calculation.

### 2.3. Estimation of $a_0^*$

When the donor side concentration is lower than  $K_m$ ,  $C_{1f_{u1}}$  becomes smaller than  $K_m$  and the efflux transport follows the first order kinetics. In the case of sequential first order permeation,  $P_{app,B-A}$  at a steady-state can be expressed as the sum of the resistance (reciprocal of permeability) from the basolateral and apical membranes (assuming the UWL and paracellular pathway are negligible),

$$\frac{1}{A_{well} P_{ep,B-A}} = \frac{1}{a_0(p_{PD} + p_{efflux})} + \frac{1}{\alpha a_2 p_{PD}} \quad (11)$$

$$p_{efflux} = \frac{J_{max}}{K_m} \quad (12)$$

On the other hand, the efflux ratio (ER) can be calculated as (see Appendix),

$$ER = \frac{P_{ep,B-A}}{P_{ep,A-B}} = 1 + \frac{p_{efflux}}{p_{PD}} \quad (13)$$

By inserting Eq. (13) in to Eq. (11) and rearranging, we obtain,

$$\frac{p_{PD}}{P_{ep,B-A}} = \frac{A_{well}}{a_0} \frac{1}{ER} + \frac{A_{well}}{\alpha a_2} \quad (14)$$

By replacing  $p_{PD}$  by the key equation of Eq. (3) to convert the ideal permeability into observable permeability, we obtain:

$$\frac{P_{app,PD,trans}}{P_{ep,B-A}} = a_2^* \frac{1}{ER} + a_0^* \quad (cf. \quad a_0^* + a_2^* = 1) \quad (15)$$

Therefore,

$$\begin{aligned} a_0^* &= \frac{P_{app,PD,trans} - P_{app,ep,A-B}}{P_{app,ep,B-A} - P_{app,ep,A-B}} \\ &= \frac{(P_{app,PD,trans} + P_{para}) - (P_{app,ep,A-B} + P_{para})}{(P_{app,ep,B-A} + P_{para}) - (P_{app,ep,A-B} + P_{para})} \end{aligned} \quad (16)$$

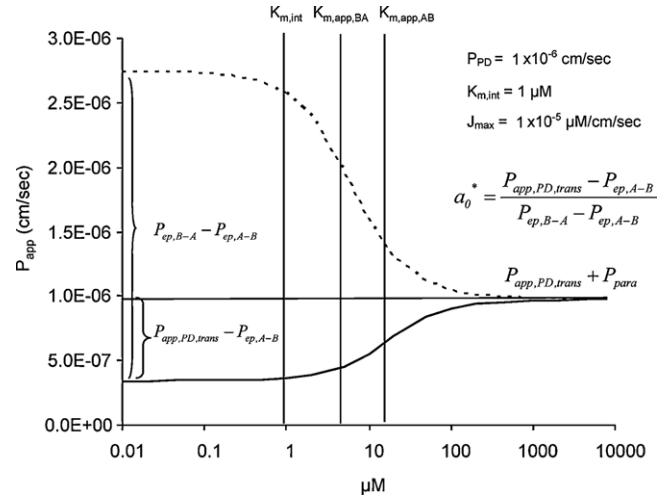


Fig. 2. Concentrations–permeability relationship of a model drug. The solid line: A to B direction. The dotted line: B to A direction. It is often difficult to concentration dependency for low solubility compounds.

$a_0^*$  reflects the asymmetric permeability of A to B and B to A directions (Fig. 2). Previously, the surface area ratio ( $a_0$  to  $a_2$ ) in Caco-2 was directly measured to be 1: 3 (Trotter and Storch, 1991). Therefore, theoretically,  $a_0^*$  should be 0.25 when no other transporter is involved or no difference in the ideal passive permeability ( $\alpha = 1$ ). The contribution of paracellular pathway permeability ( $P_{para}$ ) is cancelled out as in Eq. (16).

### 2.4. Calculation of $K_m$ and $J_{max,app}$

All calculations were performed with MS-Excel.  $K_m$  and  $J_{max,app}$  can be obtained by curve-fitting Eqs. (9) and (10) to experimental concentration–permeability curve (the least square method was used with Newton optimization (by Excel solver function)).

## 3. Results and discussion

Fig. 2 shows the theoretical concentration–permeability curve when the asymmetry of passive permeation in the apical and basolateral permeation was taken into account. The ratio of the difference between  $P_{app,A-B}$  and  $P_{app,B-A}$  and  $P_{app,PD,trans}$  corresponds to  $a_0^*$  (Eq. (16)). If the permeability–surface area product for passive permeation is higher in the basolateral membrane,  $a_0^*$  becomes less than 0.5 and the apparent  $K_m$  value becomes higher in A to B direction than in B to A direction. It should be noted that this is a theoretical curve in an idealistic case. There are several other factors which may cause a deviation from the theoretical curve (discussed in the following).

Even though simultaneous curve fitting can be used to obtain  $a_0^*$  and  $K_m$  for a specific compound simultaneously, a stepwise calculation was used in this article to explicitly describe the calculation process. As  $a_0^*$  would be a common value for various compounds if not affected by other transporters,  $a_0^*$  is first estimated by Eq. (16) for several P-gp substrates.

Step 1: Estimation of  $a_0^*$  from  $P_{app,PD,trans}$ ,  $P_{app,A-B}$  and  $P_{app,B-A}$  data at a low concentration using Eq. (16)

Step 2: Obtain  $K_m$  from concentration dependency data (curve fitting).

To neglect the effect of the unstirred water layer, permeability values of  $>30 \times 10^{-6}$  cm/s were not used (Korjamo et al., 2009; Naruhashi et al., 2003).

**Table 1**  
Permeability and membrane surface area indices in Caco-2 and MDCK-MDR1 cells.

MW	Caco-2						MDCK-MDR1					Ref.
	$P_{app,inh}$ <sup>a,b</sup>	$P_{app,A-B}$ <sup>a</sup>	$P_{app,B-A}$ <sup>a</sup>	$\alpha_0^*$	$\alpha$		$P_{app,inh}$ <sup>a,b</sup>	$P_{app,A-B}$ <sup>a</sup>	$P_{app,B-A}$ <sup>a</sup>	$\alpha_0^*$	$\alpha$	
Acebutolol	336	6.4	1.5	18	0.29	0.8	3.7	0.56	17	0.19	1.4	Troutman and Thakker (2003a,b) <sup>b</sup>
Colchicine	399	2.8	1.0	17	0.11	2.7	1.6	0.64	12	0.09	3.4	Troutman and Thakker (2003a,b) <sup>b</sup>
Cyclosporin	1203	6.9	3.0	17	0.27	0.9	4.3	0.65	10	0.41	0.5	Troutman and Thakker (2003a,b) <sup>b</sup>
Etoposide	589	3.0	1.1	14	0.15	1.9	0.66	0.30	10	0.04	9.0	Troutman and Thakker (2003a,b) <sup>b</sup>
Fexofenadine	502	1.1	0.17	14	0.06	4.9						Petri et al., 2004
Ranitidine	314	2.8	2.7	4.4	0.07	4.8	1.3	1.2	3.3	0.03	9.7	Troutman and Thakker (2003a,b) <sup>b</sup>
Rhodamine 123	381	1.7	1.4	16	0.02	16	1.2	0.98	15	0.01	26	Troutman and Thakker (2003a,b) <sup>b</sup>
Talinolol	363	15	6.7	29	0.38	0.6	2.7	0.72	23	0.09	3.4	Troutman and Thakker (2003a,b) <sup>b</sup>
Vinblastine	811	6.0	3.8	13	0.24	1.0						Lentz et al. (2000) <sup>b</sup>

<sup>a</sup>  $\times 10^{-6}$  cm/s.

<sup>b</sup> GW918 (0.5–2  $\mu$ M) was used as P-gp inhibitor.

### 3.1. Estimation of $\alpha_0^*$

To obtain  $\alpha_0^*$ , several experimental values of  $P_{app,PD,trans}$ ,  $P_{app,ep,A-B}$  and  $P_{app,ep,B-A}$  are collected from the literature (Table 1) (Lentz et al., 2000; Petri et al., 2004; Troutman and Thakker, 2003a,b). As a potent and selective inhibitor for P-gp, GW918 (0.5–2  $\mu$ M) was used in these reports (Petri et al., 2004). As shown in Table 1, similar results were obtained for both Caco-2 and MDCK-MDR1 cells. Experimental  $\alpha_0^*$  values are close to or less than 0.25 for many cases. Therefore, the product of ideal permeability and surface area for passive diffusion in the apical membrane is smaller than that in the basolateral membrane. This result is in good agreement with the apical/basolateral surface area ratio of Caco-2 cells previously reported (Trotter and Storch, 1991), though it might be counter-intuitive considering the microvilli in the apical membrane.  $\alpha_0^*$  of rhodamine 123, ranitidine and fexofenadine are significantly smaller than 0.25. When a transporter other than an apical efflux transporter is involved or when the passive permeability of a drug is sensitive to the difference in the fluidity of the membrane,  $\alpha_0^*$  could deviate from 0.25 and  $\alpha$  becomes larger than 1. However, since it was reported that the  $P_{app,ep,A-B}$  and  $P_{app,ep,B-A}$  of the present model drugs were not significantly different under the presence of an P-gp inhibitor for these drugs (Lentz et al., 2000; Petri et al., 2004; Troutman and Thakker, 2003a,b), the influence of other transporters on  $\alpha_0^*$  would be minor for this particular data set.

### 3.2. Estimation of $K_m$

The concentration– $P_{app}$  profiles of fexofenadine and rhodamine 123 in Caco-2 are shown in Fig. 3. By using a single intrinsic  $K_m$  together with  $\alpha_0^*$  values, the asymmetric concentration– $P_{app}$  profiles (A–B vs B–A) can be appropriately calculated (though  $P_{app,ep,A-B}$  showed little concentration dependency). The concentration– $P_{app}$  profiles of vinblastine in Caco-2 cells with different P-gp expression level are shown in Fig. 4. The expression level dependency of apparent  $K_m$  was also appropriately calculated using the intrinsic  $K_m$ . The intrinsic  $K_m$  showed little or no expression level dependency compared to that observed for apparent  $K_m$  (Table 2). The present  $K_m$  value of vinblastine is ca. 2 times smaller than the previously reported value by Tachibana et al. (2010) as the asymmetric passive permeation is additionally taken into account in the present study. Fexofenadine and vinblastine are also the substrate of other transporters expressed in Caco-2 cells, such as OATP (Bailey et al., 2007). The P-gp inhibitor (GW918) has not been reported to inhibit OATP (Petri et al., 2004). However, in the particular data set used in this study, since  $P_{app,ep,A-B}$  and  $P_{app,ep,B-A}$  are reported to be not significantly different under the existence of P-gp inhibitor (Petri et al., 2004; Troutman and Thakker, 2003b), it was assumed that the effect of these transporter might be minor compared to the effect of P-gp and passive transport in the Caco-2 cells used in the exper-

iments. There might be an inter-laboratory variation of expression levels of each transporter. When other active transporter(s) than P-gp contributes to the permeability of a drug, even after inhibiting P-gp, the efflux ratio should deviate from unit.

In Fig. 3, only slight increase of  $P_{app,ep,A-B}$  was observed at the highest concentration. It is often difficult to increase the donor concentration as high as 10 mM. Therefore, the absence of concentration dependency in  $P_{app,ep,A-B}$  may not be a sufficient evidence to suggest the absence of efflux transport for a drug.

In this study, the model equation was first derived based on the ideal/absolute parameters, and then converted to the practically attainable parameters. This axiomatic step-wise approach is advantageous to explicitly explain the role of various factors, such as the difference of apical and basal surface areas. In Appendix, the effect of other factors such as pH and free fraction in the donor compartment is also explicitly explained.

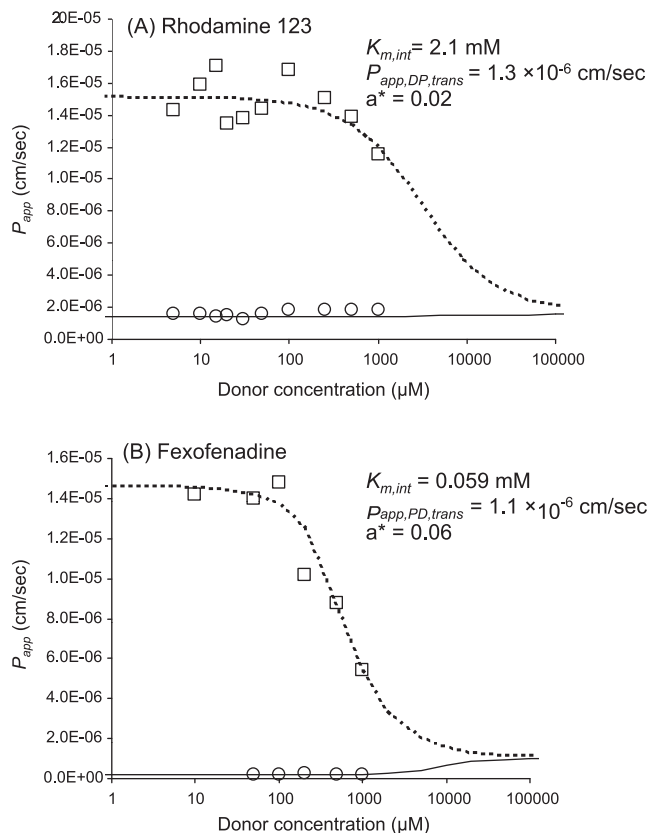


**Fig. 3.** Concentrations–permeability relationship of rhodamine 123 (A) and fexofenadine (B). Keys: circle: A to B direction, square: B to A, the solid line: simulated  $P_{app}$  in A to B direction, the dotted line: simulated  $P_{app}$  in B to A direction.

**Table 2**  
 $K_m$  and  $J_{max,app}$  for vinblastine.

Type	P-gp expression level ( $\mu\text{g}/\text{cm}^2$ ) <sup>e</sup>	Apparent $K_m$ ( $\mu\text{M}$ ) <sup>e,f</sup>	Intrinsic $K_m$ ( $\mu\text{M}$ )	$J_{max,app}$ (nM cm/sec)
KO <sup>a</sup>	8.7	30	0.86	0.10
WT <sup>b</sup>	27	81	1.43	0.26
Mid <sup>c</sup>	104	149	1.49	0.45
High <sup>d</sup>	191	323	0.98	0.68

<sup>a</sup>P-gp knock out Caco-2.<sup>b</sup>Wild type Caco-2.<sup>c</sup>Moderately P-gp induced Caco-2.<sup>d</sup>Highly P-gp induced Caco-2.<sup>e</sup>Data from Shirasaka et al. (2008).<sup>f</sup>A to B direction.

For more dynamic simulation of oral absorption of a drug such as in vivo situation, the epithelial membrane model used in this study can be numerically solved as differential equations. The steady state approximation is valid when the concentration change in the apical and basolateral side is slower compared to the time scale to establish a steady state in the cytosol. As the cytosol volume is significantly smaller than that of the intestinal fluid volume and the body fluid volume, it is appropriate to approximate that the steady state is established within a time scale faster than the time scale of the concentration change in the GI fluid. In addition, it would be appropriate to assume a sink condition in vivo, as the plasma concentration of a drug is much smaller than the concentration in the GI fluid. In the present study, the unstirred water layer in the apical side and the villi blood flow in the basolateral side were not taken into account. By using the numerical simulation, these factors can be also taken into account. However, the effect of an efflux transporter on the oral absorption of drug is suggested to be significant only for low to medium passive permeability compounds for which the UWL and the villi blood flow is not the rate determination step (Sugano et al., 2010).

Even though the three compartment model with a simple Michaelis–Menten equation (with an intrinsic  $K_m$  value) was able to explain the expression level dependency of apparent  $K_m$  values, it is well known that the P-gp has more than one binding site (Aller et al., 2009). This might have caused an expression level dependency of apparent permeability. This point should be further investigated in the future.

In conclusion, a model equation based on the steady state approximation was derived considering the asymmetric passive

diffusion in the apical and basolateral membranes. The parameter which characterizes the asymmetry of the passive diffusion,  $a_0^*$ , was found to be close to or less than 0.25, suggesting that the product of ideal passive permeability and surface area for passive diffusion in the apical membrane is smaller than that in the basolateral membrane. Asymmetrical and expression level dependent concentration–permeability profile can be appropriately represented by considering the difference of permeability–surface area product between the apical and basolateral membrane.

#### Appendix A. The mass balance equation fully considering the asymmetry of passive permeation and the undissociated and unbound fractions in each compartment

In cell monolayer permeation with an efflux transporter on the apical membrane, the mass balance in the cell compartment can be written as,

$$\frac{dM_1}{dt} = C_0 f_n f_{u0} a_0 p_{01} - C_1 f_n f_{u1} a_0 p_{10} - C_1 f_n f_{u1} a_2 p_{12} + C_2 f_n f_{u2} a_2 p_{21} - \frac{V_{max} C_1 f_{u1}}{K_m + C_1 f_{u1}} \quad (\text{A-1})$$

where  $f_n$  is the fraction of neutral charge form;  $f_u$  is the free unbound fraction;  $p$  is the ideal permeability;  $C$  is the total dissolved drug concentration in each compartment;  $a$  is the absolute surface area;  $M$  is the compound amount in each compartment;  $K_m$  is the intrinsic Michaelis–Menten constant.

Eq. (A-1) is based on some assumptions:

- (1) Only the unbound fraction can permeate the membrane (free fraction theory).
- (2) Only the undissociated molecule can passively permeate the membrane (pH partition theory).
- (3) The simple Michaelis–Menten mechanism with one binding site can represent the efflux transport.

The assumption (2) is not required for the discussion in the main text since pH is the same in all three compartments; however, it is included in this appendix to complete the theoretical steps. Furthermore,  $p$  was assumed to be passive permeability. However, the meaning of  $p$  can be expanded to any first order permeation by a transporter. These are simple practical assumptions and can be further expanded to include more complicated cases (such as passive permeation of charged molecule) (Sugano et al., 2004).

In a trans-monolayer permeation assay, the apparent permeability is calculated from the linear region of a concentration–time profile in the acceptor compartment. In this linear range, it is appropriate to assume that a steady state mass balance in the cell compartment is achieved. Therefore, the mass balance in the cell compartment ( $dM_1/dt$ ) equals zero in this time range. By rearrang-

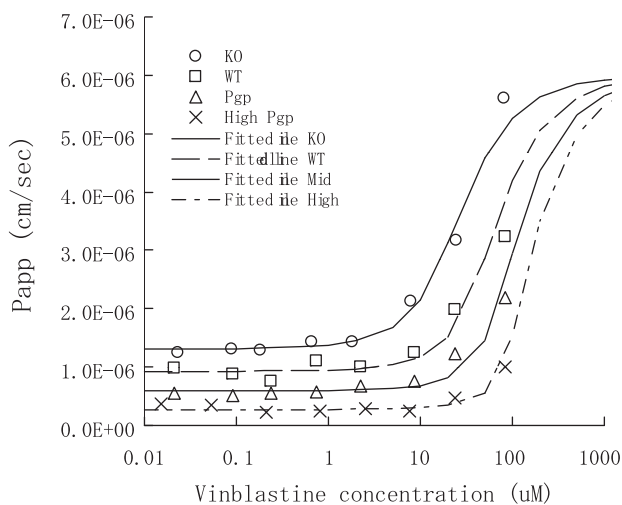


**Fig. 4.** Concentration–permeability relationship of vinblastine in Caco-2 cells with different expression levels of P-gp. The compound was applied to the apical compartment. Keys: see Table 2.

ing Eq. (A-1),

$$(C_1f_{u1})^2(f_{n1}a_0p_{10} + f_{n1}a_2p_{12}) + (C_1f_{u1})[K_m(f_{n1}a_0p_{10} + f_{n1}a_2p_{12}) + V_{\max} - (C_0f_{n0}f_{u0}a_0p_{01} + C_2f_{n2}f_{u2}a_2p_{21})] - K_m(C_0f_{n0}f_{u0}a_0p_{01} + C_2f_{n2}f_{u2}a_2p_{21}) = 0 \quad (\text{A-2})$$

This is a quadratic equation for  $C_1f_{u1}$ . By solving Eq. (A-2),  $C_1f_{u1}$  can be obtained as:

$$C_1f_{u1} = \frac{-b' + \sqrt{b'^2 - 4a'c'}}{2a'} \quad (\text{A-3})$$

$$a' = f_{n1}a_0p_{10} + f_{n1}a_2p_{12} \quad (\text{A-4})$$

$$b' = K_m(f_{n1}a_0p_{10} + f_{n1}a_2p_{12}) + V_{\max} - (C_0f_{n0}f_{u0}a_0p_{01} + C_2f_{n2}f_{u2}a_2p_{21}) \quad (\text{A-5})$$

$$c' = -K_m(C_0f_{n0}f_{u0}a_0p_{01} + C_2f_{n2}f_{u2}a_2p_{21}) \quad (\text{A-6})$$

On the other hand, from the definition of  $P_{app,A-B}$  (LHS of Eq. (A-7)) and the mass transfer into basal compartment (RHS of Eq. (A-7)), we obtain (cf. Apparent permeability values are practically defined based on the flat surface area of a cell culture well ( $A_{well}$ )):

$$C_0P_{app,A-B}A_{well} = C_1f_{n1}f_{u1}a_2p_{12} - C_2f_{n2}f_{u2}a_2p_{21} \quad (\text{A-7})$$

Similarly,

$$C_2P_{app,B-A}A_{well} = C_2f_{n2}f_{u2}a_2p_{21} - C_1f_{n1}f_{u1}a_2p_{12} \quad (\text{A-8})$$

For apical to basal permeation, assuming a sink condition in the basal side ( $C_2 = 0$ ), we obtain:

$$P_{app,ep,A-B} = \frac{1}{C_0A_{well}}f_{n1}a_2p_{12}(C_1f_{u1}) \quad (\text{A-9})$$

From Eq. (A-8) ( $C_0 = 0$ ), we obtain:

$$P_{app,ep,B-A} = \frac{1}{C_2A_{well}}(C_2f_{n2}f_{u2}a_2p_{21} - (C_1f_{u1})f_{u1}A_2p_{12}) \quad (\text{A-10})$$

In these equations,  $C_0$  and  $C_2$  are the donor concentrations for  $P_{app,A-B}$  and  $P_{app,B-A}$ , respectively. By inserting Eq. (A-3) ( $C_1f_{u1}$ ) in to Eqs. (A-9) and (A-10),  $P_{app,A-B}$  and  $P_{app,B-A}$  can be calculated. In Eqs. (A-1)–(A-10), all factors which affect the mass transfer are fully taken into account. By applying this approach, the free unbound drug concentration in the cytosol ( $C_1f_{u1}$ ) which is important for drug–drug interaction prediction can be also calculated. As the concentration gradient is the driving force for passive diffusion of a drug,  $C_1f_{n1}f_{u1}$  is always lower than the donor concentration of undissociated unbound drug (i.e.,  $C_0f_{n0}f_{u0}$  for A to B direction). For example, in the case of cimetidine ( $pK_a = 6.9$ ), considering the difference in pH (pH 6.5 in the apical side and pH 7.0–7.4 in the cytosol) and  $a_0^* = 0.25$ , the  $C_1f_{u1}$  in the intestinal epithelial cells would be ca. 1/10 of the apical side (luminal) concentration. By using this value and the actual intestinal fluid volume (ca. 100–250 mL), the drug–drug interaction by cimetidine via CYP3A4 in the intestinal epithelial cells can be appropriately estimated (previously, an operational fluid volume of ca. 1900 mL was used for this calculation) (Tachibana et al., 2009).

However, in some in vitro experiments, simple experimental conditions are often used, such as the iso pH condition and no additives in the donor and acceptor chambers. In the following, the equations for simple cases are discussed by simplifying Eqs. (A-1)–(A-10).

### A.1. Absence of permeability normalization by the cytosol pH

It is often discussed that, as the cytosol pH is maintained at a constant value of pH 7.0–7.4, the donor pH should not have any impact on permeability, even though this is inconsistent with the experimental observations. This controversy is easily explained as follows.

In the absence of efflux transporters, Eqs. (A-1) and (A-2) can be simplified as (assuming a sink condition in the basal side ( $C_2 = 0$ )):

$$C_0f_{n0}f_{u0}a_0p_{01} - C_1f_{n1}f_{u1}(a_0p_{10} + a_2p_{12}) = 0 \quad (\text{A-11})$$

By rearranging this equation, we obtain:

$$C_1f_{u1} = \frac{f_{n0}f_{u0}}{f_{n1}} \frac{a_0p_{01}}{(a_0p_{10} + a_2p_{12})} C_0 \quad (\text{A-12})$$

By inserting Eq. (A-12) into Eq. (A-9),

$$P_{app,ep,A-B} = \frac{f_{n1}a_2p_{12}}{C_0A_{well}} \frac{f_{n0}f_{u0}}{f_{n1}} \frac{a_0p_{01}}{(a_0p_{10} + a_2p_{12})} C_0 = f_{n0}f_{u0}P_{app,PD,trans,int} \quad (\text{A-13})$$

$$P_{app,PD,trans,int} = \frac{1}{A_{well}} \frac{a_0a_2p_{01}p_{12}}{(a_0p_{10} + a_2p_{12})}$$

Since the ideal permeability and absolute surface area are constant, this equation suggests that  $P_{app,ep,A-B}$  only depends on the unbound fraction of undissociated species in the donor compartment ( $f_{n0}f_{u0}$ ), but not those in the cytosol compartment as  $f_{n1}f_{u1}$  does not appear in this equation. In other words, even though pH is maintained at pH 7.4 and the unbound fraction of a drug could be significantly smaller than 1 in the cytosol,  $P_{app,ep,A-B}$  at the steady state solely depends the pH and unbound fraction of a drug in the donor compartment (therefore, there is no controversy between the pH partition theory and the constant cytosol pH). This is in good agreement with the experimental observations (Avdeef et al., 2005; Neuhoff et al., 2006; Yamashita et al., 2000). Furthermore, Eq. (A-13) suggests that even if the product of permeability and surface area in the apical membrane is larger than that in the basolateral membrane (i.e., the basolateral membrane is the larger barrier), only the apical side pH affects apparent permeability (i.e., we do not have to postulate the apical membrane being the largest barrier to explain the pH dependency of the experimental data). It should be noted that  $P_{app,PD,trans,int}$  is usually referred to as “intrinsic” permeability (of undissociated species) in the literature. To avoid complication in this article, the word “ideal” was used rather than “intrinsic” to refer the permeability based on an absolute membrane surface area and a single leaf of a membrane.

By deriving  $P_{app,B-A}$  in the same way as Eq. (A-13) and taking the ratio, under iso pH and no additive condition ( $f_{n0} = f_{n2} (=f_{n1})$ ,  $f_{u0} = f_{u2}$ ), we obtain:

$$\frac{P_{app,B-A}}{P_{app,A-B}} = \frac{f_{n2}f_{u2}(1/A_{well})(a_0a_2p_{10}p_{21}/(a_0p_{10} + a_2p_{12}))}{f_{n0}f_{u0}(1/A_{well})(a_0a_2p_{12}p_{01}/(a_0p_{10} + a_2p_{12}))} = \frac{p_{10}p_{21}}{p_{01}p_{12}} \quad (\text{A-14})$$

Many drugs showed that  $P_{app,ep,A-B}$  and  $P_{app,ep,B-A}$  become the same value under perfect inhibition of carrier mediated transports (i.e.,  $P_{app,B-A}/P_{app,A-B} = 1$ ) (Troutman and Thakker, 2003a,b). The probability that  $p_{10}/p_{12}$  and  $p_{21}/p_{01}$  coincidentally cancels out to give an unit value would be very low. Therefore, it would be appropriate to assume that passive permeability in the influx and efflux directions (i.e., 0 to 1 and 1 to 0 direction) in the same membrane are the same. At the same time, Eq. (A-14) also indicated that  $P_{app,B-A}/P_{app,A-B} = 1$  does not mean  $a_0 = a_2$ .

## A.2. Efflux ratio (ER)

When  $C_{1f_{u1}} < K_m$ , an efflux transport becomes first order.

$$\frac{J_{\max} C_{1f_{u1}}}{K_m + C_{1f_{u1}}} \approx \frac{J_{\max}}{K_m} C_{1f_{u1}} = p_{\text{efflux}} C_{1f_{u1}} \quad (\text{A-15})$$

where  $p_{\text{efflux}}$  is the ideal efflux permeability. By inserting Eq. (A-15) into Eq. (A-1) and rearranging, we obtain (under iso pH and no additive condition ( $f_{n0} = f_{n2}$  ( $=f_{n1}$ ),  $f_{u0} = f_{n2}$ )):

$$C_{1f_{u1}} = \frac{C_0 a_0 p_{PD} + C_2 a_2 \alpha p_{PD}}{a_0 p_{PD} + a_2 \alpha p_{PD} + a_0 p_{\text{efflux}}} \quad (\text{A-16})$$

For apical to basal permeation, assuming a sink condition in the basal side ( $C_2 = 0$ ) and no paracellular pathway, by inserting Eq. (A-16) into Eq. (A-9), we obtain:

$$P_{\text{app,ep,A-B}} = \frac{1}{A_{\text{well}}} \frac{\alpha a_0 a_2 p_{PD}^2}{a_0 p_{PD} + a_2 \alpha p_{PD} + a_0 p_{\text{efflux}}} \quad (\text{A-17})$$

Similarly we obtain,

$$P_{\text{app,ep,B-A}} = \frac{\alpha a_2 p_{PD}}{A_{\text{well}}} \left( 1 - \frac{a_2 \alpha p_{PD}}{a_0 p_{PD} + a_2 \alpha p_{PD} + a_0 p_{\text{efflux}}} \right) \quad (\text{A-18})$$

Therefore

$$\text{ER} = \frac{P_{\text{app,ep,B-A}}}{P_{\text{app,ep,A-B}}} = 1 + \frac{p_{\text{efflux}}}{p_{PD}} \quad (\text{A-19})$$

## References

- Aller, S.G., Yu, J., Ward, A., Weng, Y., Chittaboina, S., Zhuo, R., Harrell, P.M., Trinh, Y.T., Zhang, Q., Urbatsch, I.L., Chang, G., 2009. Structure of P-glycoprotein reveals a molecular basis for poly-specific drug binding. *Science* (Washington, DC, U.S.) 323, 1718–1722.
- Avdeef, A., Artursson, P., Neuhoff, S., Lazorova, L., Grasjoe, J., Tavelin, S., 2005. Caco-2 permeability of weakly basic drugs predicted with the Double-Sink PAMPA pKfluxa method. *Eur. J. Pharm. Sci.* 24, 333–349.
- Bailey, D.G., Dresser, G.K., Leake, B.F., Kim, R.B., 2007. Naringin is a major and selective clinical inhibitor of organic anion-transporting polypeptide 1A2 (OATP1A2) in grapefruit juice. *Clin. Pharmacol. Ther.* 81, 495–502.
- Garmire, L.X., Garmire, D.G., Hunt, C.A., 2007. An in silico transwell device for the study of drug transport and drug–drug interactions. *Pharm. Res.* 24, 2171–2186.
- Garmire, L.X., Hunt, C.A., 2008. In silico methods for unraveling the mechanistic complexities of intestinal absorption: metabolism–efflux transport interactions. *Drug Metab. Dispos.* 36, 1414–1424.
- Heikkinen, A.T., Moenkkonen, J., Korjamo, T., 2010. Determination of permeation resistance distribution in in vitro cell monolayer permeation experiments. *Eur. J. Pharm. Sci.* 40, 132–142.
- Horie, K., Tang, F., Borchardt, R.T., 2003. Isolation and characterization of Caco-2 subclones expressing high levels of multidrug resistance protein efflux transporter. *Pharm. Res.* 20, 161–168.
- Korjamo, T., Heikkinen, A.T., Moenkkonen, J., 2009. Analysis of unstirred water layer in in vitro permeability experiments. *J. Pharm. Sci.* 98, 4469–4479.
- Korjamo, T., Kemilainen, H., Heikkinen, A.T., Moenkkonen, J., 2007. Decrease in intracellular concentration causes the shift in  $K_m$  value of efflux pump substrates. *Drug Metab. Dispos.* 35, 1574–1579.
- Kwon, H., Lionberger, R.A., Yu, L.X., 2004. Impact of P-glycoprotein-mediated intestinal efflux kinetics on oral bioavailability of P-glycoprotein substrates. *Mol. Pharm.* 1, 455–465.
- Lentz, K.A., Polli, J.W., Wring, S.A., Humphreys, J.E., Polli, J.E., 2000. Influence of passive permeability on apparent P-glycoprotein kinetics. *Pharm. Res.* 17, 1456–1460.
- Naruhashi, K., Tamai, I., Li, Q., Sai, Y., Tsuji, A., 2003. Experimental demonstration of the unstirred water layer effect on drug transport in caco-2 cells. *J. Pharm. Sci.* 92, 1502–1508.
- Neuhoff, S., Artursson, P., Zamora, I., Ungell, A.-L., 2006. Impact of extracellular protein binding on passive and active drug transport across caco-2 cells. *Pharm. Res.* 23, 350–359.
- Petri, N., Tannergren, C., Rungstad, D., Lennernaes, H., 2004. Transport characteristics of fexofenadine in the Caco-2 cell model. *Pharm. Res.* 21, 1398–1404.
- Rostami-Hodjegan, A., Tucker, G.T., 2007. Simulation and prediction of in vivo drug metabolism in human populations from in vitro data. *Nat. Rev. Drug Discov.* 6, 140–148.
- Saitoh, R., Sugano, K., Takata, N., Tachibana, T., Higashida, A., Nabuchi, Y., Aso, Y., 2004. Correction of permeability with pore radius of tight junctions in Caco-2 monolayers improves the prediction of the dose fraction of hydrophilic drugs absorbed by humans. *Pharm. Res.* 21, 749.
- Shirasaka, Y., Sakane, T., Yamashita, S., 2008. Effect of P-glycoprotein expression levels on the concentration-dependent permeability of drugs to the cell membrane. *J. Pharm. Sci.* 97, 553–565.
- Sugano, K., 2009. Theoretical investigation of passive intestinal membrane permeability using Monte Carlo method to generate drug like molecule population. *Int. J. Pharm.* 373, 55–61.
- Sugano, K., Kansy, M., Artursson, P., Avdeef, A., Bendels, S., Di, L., Ecker, G.F., Faller, B., Fischer, H., Gerebtzoff, G., Lennernaes, H., Senner, F., 2010. Coexistence of passive and carrier-mediated processes in drug transport. *Nat. Rev. Drug Discov.* 9, 597–614.
- Sugano, K., Nabuchi, Y., Machida, M., Asoh, Y., 2004. Permeation characteristics of a hydrophilic basic compound across a bio-mimetic artificial membrane. *Int. J. Pharm.* 275, 271–278.
- Sugano, K., Takata, N., Machida, M., Saitoh, K., Terada, K., 2002. Prediction of passive intestinal absorption using bio-mimetic artificial membrane permeation assay and the paracellular pathway model. *Int. J. Pharm.* 241, 241–251.
- Tachibana, T., Kato, M., Watanabe, T., Mitsui, T., Sugiyama, Y., 2009. Method for predicting the risk of drug–drug interactions involving inhibition of intestinal CYP3A4 and P-glycoprotein. *Xenobiotica* 39, 430–443.
- Tachibana, T., Kitamura, S., Kato, M., Mitsui, T., Shirasaka, Y., Yamashita, S., Sugiyama, Y., 2010. Model analysis of the concentration-dependent permeability of P-gp substrates. *Pharm. Res.* 27 (3), 442–446.
- Trotter, P.J., Storch, J., 1991. Fatty acid uptake and metabolism in a human intestinal cell line (Caco-2): comparison of apical and basolateral incubation. *J. Lipid Res.* 32, 293–304.
- Troutman, M.D., Thakker, D.R., 2003a. Efflux ratio cannot assess P-glycoprotein-mediated attenuation of absorptive transport: asymmetric effect of P-glycoprotein on absorptive and secretory transport across Caco-2 cell monolayers. *Pharm. Res.* 20, 1200–1209.
- Troutman, M.D., Thakker, D.R., 2003b. Novel experimental parameters to quantify the modulation of absorptive and secretory transport of compounds by P-glycoprotein in cell culture models of intestinal epithelium. *Pharm. Res.* 20, 1210–1224.
- Yamashita, S., Furubayashi, T., Kataoka, M., Sakane, T., Sezaki, H., Tokuda, H., 2000. Optimized conditions for prediction of intestinal drug permeability using Caco-2 cells. *Eur. J. Pharm. Sci.* 10, 195–204.
- Yang, J., Jamei, M., Yeo, K.R., Tucker, G.T., Rostami-Hodjegan, A., 2007. Prediction of intestinal first-pass drug metabolism. *Curr. Drug Metab.* 8, 676–684.